PAPER • OPEN ACCESS

Formation of metastable zirconium oxides using pulsed laser deposition of ZrO based target

View the article online for updates and enhancements.

Formation of metastable zirconium oxides using pulsed laser deposition of ZrO based target

Tomáš Křenek[1], Petr Mikysek[2,3], Michal Pola[1], Lukáš Vála[1], Estela Melaré[5], Věra Jandová[4], Veronika Vavruňková[1], David Rieger[1]

[1] University of West Bohemia, Research Centre New Technologies 30614 Plzeň, Czech Republic

[2] The Czech Academy of Sciences, Institute of Geology, Rozvojová 269, 165 00 Prague 6, Czech Republic

[3] Masaryk University, Faculty of Science, Institute of Geological Sciences, Kotlářská 2, 611 37 Brno, Czech Republic

[4] Institute of Chemical Process Fundamentals, Czech Academy of Sciences, Rozvojova 135, 160 00 Prague 6, Czech Republic

[5] Federal University of São Carlos, Department of Chemistry, Interdisciplinary Laboratory of Electrochemistry & Ceramics (LIEC), Rodovia Washington Luis, Km 235, SP-310, Monjolinho, 13565905 - São Carlos, SP, Brasil

E-mail: tkrenek@ntc.zcu.cz

Abstract

There is a growing interest about the possibilities for preparation of various zirconium oxides from scientific as well as application point of view. Laser ablation of solid target consisting of sintered grains of metallic hexagonal Zr_3O and monoclinic ZrO_2 results in evaporation of Zr, O species (ions, atoms) and subsequent deposition of Zr-O film. Ta and Cu have been used as substrates. The films were analyzed by SEM-EDX, Raman and FTIR spectroscopy and X-ray diffraction. SEM analysis revealed µm/sub-µm sized roundshape and ring-like objects on continuous coat. Using Raman spectroscopy broad peaks which can suggest partial laser induced amorphization of Zr-O deposits were detected. FTIR spectroscopy shows bands which are assignable to Zr-O vibration of nanostructured zirconia. X-ray diffraction analysis provides more explicit assignment of deposited phases where the deposit on Ta exhibits presence of monoclinic ZrO_2, oxygen deficient rhombohedric Zr_3O and interestingly indicates presence of high-pressure orthorhombic ZrO_2 phase. The coat on Cu consists of monoclinic ZrO_2, rhombohedric Zr_3O, and metastable tetragonal ZrO_2 phase.

1. Introduction

There is a growing interest about the properties of zirconium oxides in a wide range of applications. Zr and ZrO_2 have been proved as useful materials for orthopedic applications because ZrO_2 possesses high hardness, wear and corrosion resistance, and good biocompatibility [1–4]. Though ZrO_2 is mostly considered as bioinert material also its bioactivity is possible to enhanced [5]. ZrO_2 belongs among wide band gap (with band gap of ~5 eV) n-type semiconductors which represent suitable photocatalysts for the decomposition of water pollution [6-11]. Among these wide band gap semiconductors, especially ZrO_2 nanoparticles have been attracted considerable attention because of their various potential applications [6], and also play a significant role in photocatalysis research due to their high surface to

volume ratio [12]. Nanostructured zirconia represents promising material also because of its unique optical and electrical properties as well as other potential applications in transparent optical devices, oxygen sensors, fuel cells, electrochemical capacitor electrodes, and advanced ceramics [13-17]. The applications of zirconia strongly depend on both crystal structure and phase transformations [15-17].

Pure Zr possesses two crystalline modifications: hcp crystal structure (α-Zr) which transforms to the bcc crystal structure (β-Zr) above 889°C [18]. Both hcp and bcc polymorphs of Zr possess significantly high oxygen solubility. The β-Zr is able to dissolve 10.5 at% oxygen at high temperatures, whereas the solubility of α-Zr achieves values as high as 28.6–35 at% of oxygen. Exceedance of the solubility limit of oxygen leads to the formation of ZrO_2 which crystallize in three polymorphs according the temperature: the monoclinic α-ZrO_2 phase is stable below 1000°C, the intermediate tetragonal β-ZrO_2 phase is stable at 1200°C and is transformed to a cubic γ -ZrO_2 phase above 2285 °C [19]. Moreover to γ -, β-, and α-ZrO_2, at least two orthorhombic phases are stabilized at high pressure [20]. Contrary to well described ZrO_2 there is not fully known stable bulk form of ZrO.

Here we report on pulsed laser deposition of the Zr-O target consisting of monoclinic ZrO_2 and hexagonal Zr_3O sintered grains. The laser ablative deposition represents challenging method for preparation of smooth and nanostructured films as well as nanosized particles from elemental, inorganic and organic bulk materials [eg. 21, 22]. Thermodynamically non-equilibrium conditions of laser ablation [21] are challenging for deposition of metastable Zr-O phases.

2. Experimental

A 3rd harmocnic of pulsed Nd:YAG laser (model Q SMART 850, base wavelength: 1064 nm, used wavelength: 355 nm, energy per pulse: 180 ± 5 mJ, pulse duration: 10 ns, repetition rate: 10 Hz) was used for ablation of a ZrO target. The irradiation was focused by lens (f = 15 cm) on the spot area of 0.02 cm^2. Laser irradiation experiments were carried out in a simple tubular Pyrex reactor (70 mL in volume) continuously pumped to high vacuum by using a turbomolecular source (base pressure 5 x 10^{-2} Pa). The reactor was furnished with borosilicate glass windows. The duration of irradiation was 6 minutes. The target of ZrO pellet with diameter 14 mm and height 5 mm was positioned vertically in the center of the reactor and the substrate was situated perpendicularly above the target. The tantalum and copper foils were used as a substrate. For each sample deposition, first the vacuum chamber is opened and the clean substrate is placed inside of the Pyrex chamber. Then, the reactor is closed and the pressure is lowered. After the irradiation the pressure is increased up to atmospheric, the chamber is opened, the sample with the resulting coats is taken for examination and a new sample is placed.

Raman spectra were obtained using a DXR Raman microscope with Diode-pumped solid state laser emitting at 532 nm using high resolution gratings working in the range of 50 – 1800 cm^{-1} and spectral resolution 2 cm^{-1} FWHM.

Infrared absorbance spectra were performed on the Nicolet 380 FTIR spectrometer in the range of 650–4000 cm^{-1} using the ATR (attenuated total reflection) accessory with trapezoidal silicon crystal with a beveled edge of 45 degree. ATR technique offers a high sensitivity of absorbance measurements due to special data acquisition by multi-passing the investigated thin films by IR radiation.

X-ray diffraction investigation was carried out with a Bruker D8 Discover diffractometer equipped with a silicon-strip linear LynxEye detector and a focusing germanium primary monochromator of Johansson type providing Cu$K\alpha_1$ radiation (λ = 1.54056 Å). Data for mineral identification were collected in the 2θ range of 20–125° with a step size of 0.016° and a counting time of 8 second at each step, and detector angular opening of 3.757°. The phase identification was performed with Diffrac.Eva software v4.2.2 and ICDD PDF-2 database (Bruker AXS GmbH, Karlsruhe, Germany; 2011–2016). ZrO target represents commercially available product: Zirconium monooxide ZrO tablets (umicore).

3. Results and discussion

The UV laser irradiation of ZrO target in vacuum leads to ablation and creation of visible bluish luminescence zone suggesting ionization. The laser ablation results in the deposition of the coat which exhibit similar interference appearance on both Ta as well as Cu substrate (Fig. 1). Ta has been selected as an inert substrate and Cu as a substrate with reactive potential.
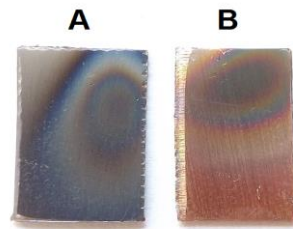
Fig. 1 The coated Ta (a), Cu (b) substrates.

The SEM images of the deposit on Ta (Fig.2 A) reveal μm/sub-μm sized roundshape and ringlike objects on continuous coat. The elemental mapping (Fig. 2 B) shows homogenous distribution of Zr with higher concentration in μm-sized particles. The deposit morphology on Cu substrate (Fig. 2 C) exhibits spherical particles with the size spanning from tens of nm up to units of μm. Elemental mapping (Fig. 2 D) depicts large shapeless agglomerates with high Zr concentration whereas the continuous surrounding seems to possess lower Zr content compared to the coat on Ta. The presence of larger shapeless/ringlike objects is in accordance with vaporized and plasma-produced clusters, and liquid droplets expelled from the target surface and quenched upon deposition. The roundshaped smaller particles indicate the rapid cooling of the solidifying droplets, which may occur in a metastable/amorphous state. SEM-EDX analysis provides the ratio of presented elements (Zr, O, Ta/Cu) where is detected excess of oxygen in Zr:O ratio which can indicate small oxidation of the substrates.
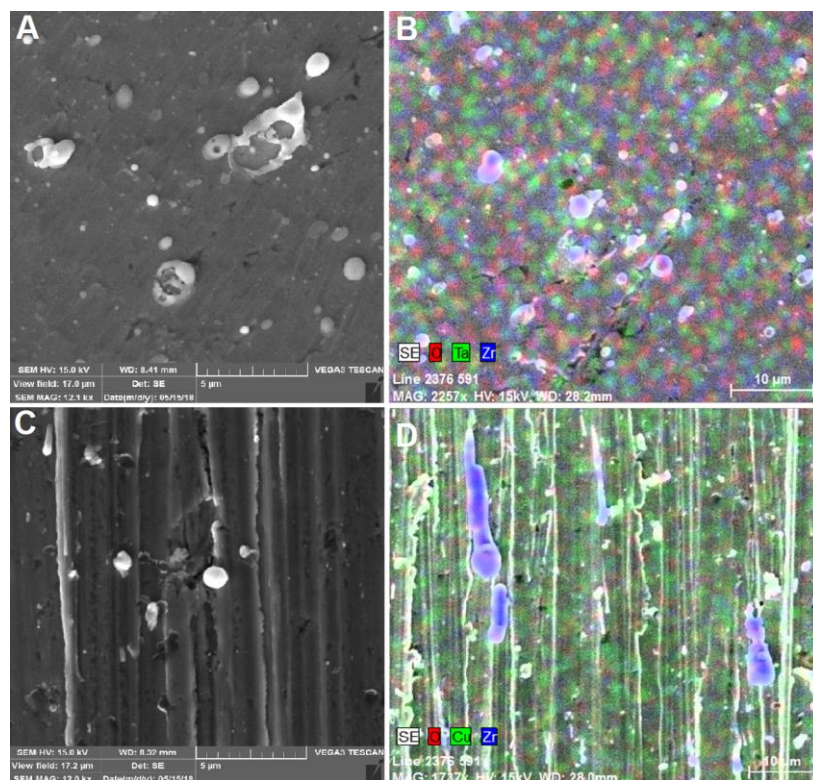

Fig. 2 SEM images of coats deposited on Ta (A) and Cu (C);
elemental mapping on Ta (B) and Cu (D)

Raman spectroscopy analysis revealed the presence of two phases in original target (Fig. 3 A). The target consists of sintered grains where one kind of the grains does not possess any vibrational peaks and thus can belongs to metallic Zr or solid solution of Zr and O and the second one whose peaks agrees with monoclinic ZrO_2 [23, 24]. The peak position slightly differs compared to literature [23, 24] which can

be caused by stress in the target which was prepared obviously by sintering under the press. The Raman spectroscopy of Zr-O coat on Ta and Cu (Fig. 3 B) shows different features compared to original target which suggest that some phase transformation was carried out. The deposit on Ta reveals the broad peaks centered at ~ 167 cm^{-1}, 241 cm^{-1}, 620 cm^{-1}. The most significant broad peaks of the coat on Cu are positioned at ~ 290 cm^{-1}, 620 cm^{-1}. The peak at 620 cm^{-1} is similar for both Ta and Cu substrate whereas to position of other peaks varies. The broad peaks occur in the same regions like the sharp peaks of crystalline monoclinic ZrO_2 in original target. From the broad shape of the peaks we can tentatively conclude that partial laser induced amorphization of Zr-O phase took place.
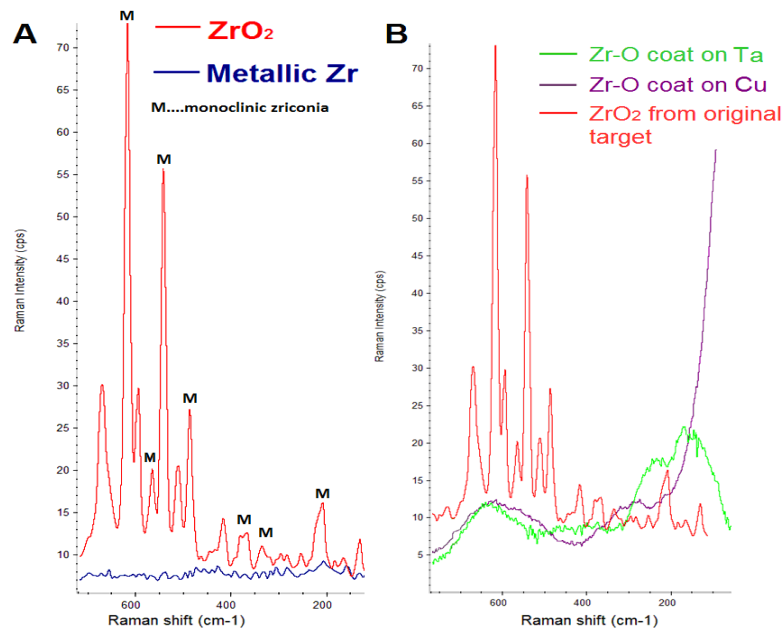

Fig.3 Raman spectroscopy of the original target (A)
and of the coats on Ta and Cu substrates (B)

FTIR spectra exhibit very similar features for the deposits on Ta and Cu (Fig. 4). It revealed presence of bands at 630, 654 and 842 cm^{-1} which is assigned to strong stretching vibrations of the Zr-O group [25]. The vibration band around 1652 cm^{-1} is attributed to Zr-OH vibration [25] and the absorbance band at around 3300 cm^{-1} agrees with the adsorbed water which is consistent with the published FTIR spectra of nano-ZrO_2 [26].
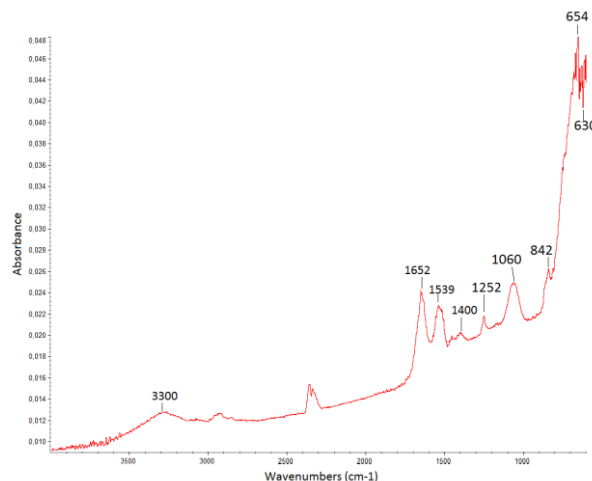

Fig. 4 Typical FTIR spectrum for Zr-O coat on Ta and Cu

XRD of the ablated pellet exhibits in agreement with Raman spectroscopy presence of two phases: monoclinic ZrO_2 and hexagonal Zr_3O. Oxygen deficient hexagonal Zr_3O represents solid solution of O in hcp α-Zr. The weight fraction of present phase corresponds with approximately 1/3 of monoclinic ZrO_2 and 2/3 of hexagonal Zr_3O. XRD analysis of the deposit on Ta (Fig. 5) shows intensive peaks corresponding with cubic body centered Ta of the substrate. In the detail of the XRD spectrum less intensive diffraction peaks of the polycrystalline coat are visible. The peaks are clearly assignable to monoclinic ZrO_2 and to oxygen deficient rhombohedric Zr_3O. Moreover XRD analysis suggests interestingly also the presence of orthorhombic ZrO_2 phase which is stabilized only under the high pressure [20]. The brief crystallographic description of detected phases summarizes Tab.1.
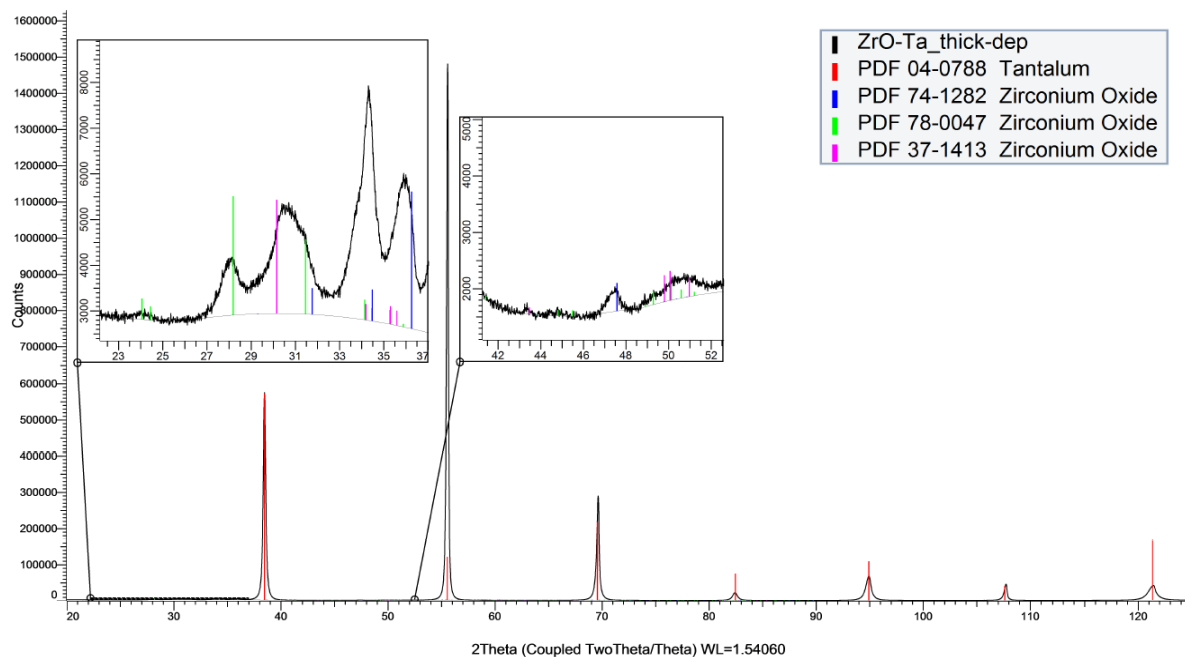

Fig. 5 XRD of Zr-O coat on Ta

Tab. 1 List of phases of the coat on Ta assigned using XRD

Pattern #	Compound Name	Formula	System	Space Group
PDF 04-0788	Tantalum	Ta	Cubic	Im3m (229)
PDF 74-1282	Zirconium Oxide	Zr3O	Rhombo.H.axes	R-3c (167)
PDF 78-0047	Zirconium Oxide	ZrO2	Monoclinic	P21/c (14)
PDF 37-1413	Zirconium Oxide	ZrO2	Orthorhombic	P212121 (19)

XRD of Zr-O coat on Cu (Fig. 6) revealed the most intensive peaks belonging to cubic Cu of the substrate. Less intensive peaks of the coat are in good agreement with monoclinic ZrO_2 and to oxygen deficient rhombohedric Zr_3O as in the case of Ta substrate. However in coat on Cu XRD indicates the peaks corresponding with tetragonal ZrO_2 phase which is considered as unstable phase under the room temperature. Contrary to the coat on Ta there is no evidence of high-pressure orthorhombic ZrO_2 polymorph. Summarization of the phases detected in the coat on Cu is given in Tab. 2.

In case of both deposits the assignment of monoclinic ZrO_2 and rhombohedric Zr_3O is unambiguous however the clear confirmation of high-pressure orthorhombic and unstable tetragonal structure should be investigated and clearly confirmed by next analytical methods such as back-scattered electrons and/or electron diffraction.
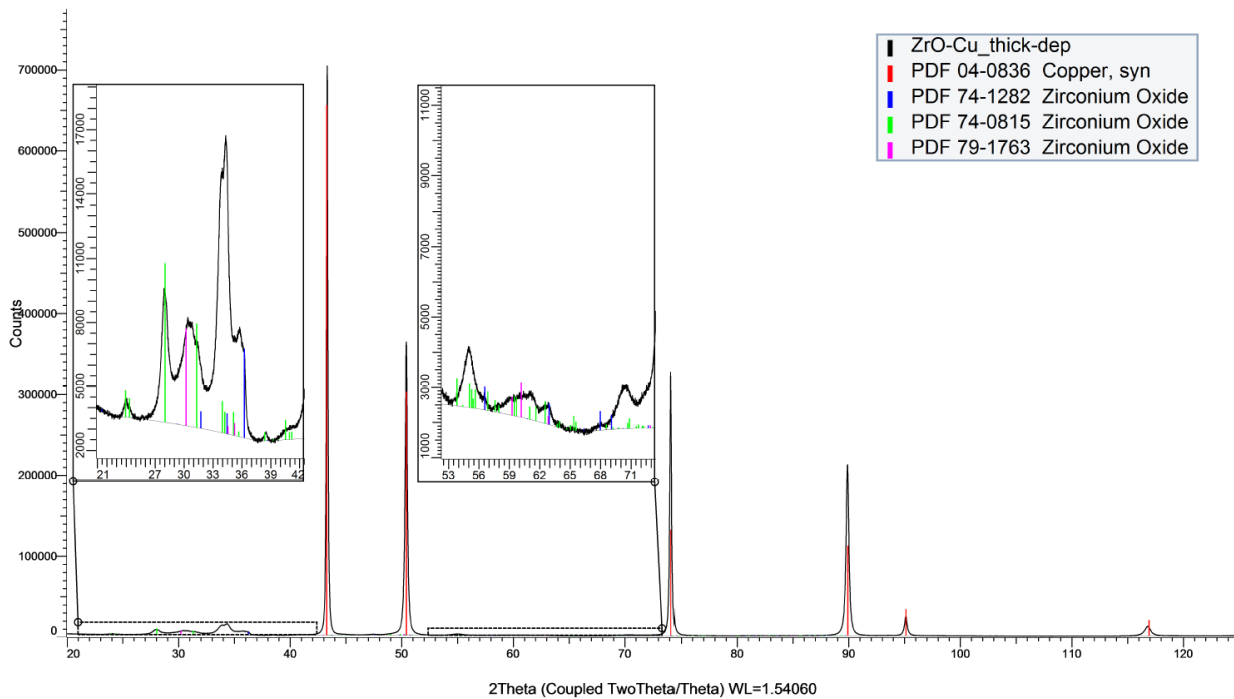
Fig.6 XRD of Zr-O coat on Cu

Tab. 2 List of phases of the coat on Cu assigned using XRD

Pattern #	Compound Name	Formula	System	Space Group
PDF 04-0836	Copper, syn	Cu	Cubic	Fm-3m (225)
PDF 74-1282	Zirconium Oxide	Zr3O	Rhombo.H.axes	R-3c (167)
PDF 74-0815	Zirconium Oxide	ZrO2	Monoclinic	P21/c (14)
PDF 79-1763	Zirconium Oxide	ZrO2	Tetragonal	P42/nmc (137)

These complementary analyses are in line with the deposition of monoclinic ZrO_2 and rhombohedric Zr_3O in case of both Ta as well as Cu coats. Moreover XRD indicates high-pressure orthorhombic ZrO_2 phase on Ta and metastable tetragonal ZrO_2 on Cu. The laser induced formation of high-pressure polymorph has been previously published for eg. orthorhombic Fe_3O_4 nanograins [27] or high-pressure Ga nanostructures [28].

   These results are consistent with rapid evaporation of both hexagonal Zr_3O and monoclinic ZrO_2 from an irradiated original target which results in intermixing events of atomic/ionic species of Zr and O in the gas phase and subsequent rapid deposition of the multi-phase structure containing also metastable zirconium oxides.

4. Conclusion
Laser ablation of the target based on sintered grains of Zr and ZrO_2 allows evaporation/ionization of present species and following deposition of Zr-O coats. The deposits on Ta and Cu exhibits roundshape and ringlike particles whose sizes span from nm up to units of μm. Raman and FTIR spectroscopy suggested formation of nanostructured partially amorphous Zr-O films. X-ray diffraction reveals formation of monoclinic ZrO_2 and rhombohedric Zr_3O on both Ta and Cu substrate. Moreover XRD suggests formation of high-pressure ortorhombic ZrO_2 phase on Ta and metastable tetragonal ZrO_2 on Cu. These results show that intermixing events in the gas phase together with highly non-equilibrium conditions of laser ablation are favorable for the deposition of various metastable Zr-O phases.

References

[1]   Spector M, Ries M D, Bourne R B, Sauer W S, Long M, Hunter G 2001 *J. Bone Joint Surg.* **83** 80

[2]   Ferraris M, Verne E, Appendino P, Moisescu C, Krajewski A, Ravaglioli A, Piancastelli A 2000 *Biomaterials* **21** 765

[3]   Suzuki T, Fujibayashi S, Nakagawa Y, Noda I, Nakamura T 2006 *Biomaterials* **27** 996

[4]   Uchida M, Kim H M, Kokubo T, Nawa M, Asano T, Tanaka K, Nakamura T 2002 *Jour. Biomed. Mater. Res.* **60** 277

[5]   Zhang L, Han Y 2011 *Materials Science and Engineering C* **31** 1104

[6]   Gröttrup J, Schütt F, Smazna D, Lupana O, Adelung R, Mishra Y K 2017 *Ceram. Int.* **43** 14915 http://dx.doi.org/10.1016/j.ceramint.2017.08.008

[7]   Mishra Y K, Adelung R 2018 *Mater. Today* http://dx.doi.org/10.1016/j.mattod.2017.11.003

[8]   Gröttrup J, Paulowicz I, Schuchardt A, Kaidas V, Kaps S, Lupan O, Rainer Adelung R, Mishra Y K 2016 *Ceram. Int.* **42** 8664

[9]   Babu B, Mallikarjuna K, Reddy Ch V, Park J 2016 *Mater. Lett.* **176** 265

[10] Reddy Ch V, Babu B, Shim J 2017 *Mater. Sci. Eng. B.* **22** 131

[11] Davar F, Loghman-Estarki M R 2014 *Ceram. Int.* **40** 8427

[12] Renuka L, Anantharaju K S, Sharma S C, Nagabhushana H, Vidya Y S, Nagaswarupa H P, Prashantha S C 2017 *J. Alloy. Compd.* **695** 382

[13] Jamali H, Shoja-Razavi R, Mozafarinia R, Ahmadi-Pidani R, Loghman-Estarki M R 2012 *Curr. Nanosci.* **8** 402

[14] Loghman-Estarki M R,et al. 2014 *Ceram. Int.* **40** 3721

[15] Salavati-Niasari M, Dadkhah M 2009 *Polyhedron* **28** 3005

[16] Loghman-Estarki M R,et al. 2014 *Ceram. Int.* **40** 1405

[17] Davar F, Hassankhani A, Loghman-Estarki M R 2013 *Ceram. Int.* **39** 2933

[18] Abriata J P, Garc´es J, Versaci R 1986 *Bull. Alloy Phase Diagrams* **7** 116

[19] Atkinson A 1985 *Rev. Mod. Phys.* **57** 437

[20] Bouvier P, Djurado E, Lucazeau G, Le Bihan T 2000 *Phys. Rev. B* **62** 8731

[21] Chrisey D B, Hubler G K 1994 Pulsed Laser Deposition of Thin Films *Wiley* New York

[22] Geohegan D, Stuke M 1995 *MRS Symp. Proc.* **55**

[23] Kurpaska L et al. 2015 *Journal of Nuclear Materials* **466** 460

[24] Keramidas V G, White W B 1974 *Journal of The American Ceramic Society* **57** (1)

[25] Kolvari E, Koukabi N, Hosseini M M, Vahidian M, Ghobadi E 2016 *RSC Adv.* **6** 7419

[26] Chakravarty R, Shukla R, Ram R, Tyagi A, Dash A, Venkatesh M 2010 *Chromatin* **72** 875

[27] Pola J, Gondal M A, Urbanová M, Pokorná D, Masoudi H M, Bakardjieva S, Bastl Z, Šubrt J, Siddiqui M N 2012 *Journal of Photochemistry and Photobiology A: Chemistry* **243** 33

[28] Pokorna D, Urbanova M, Bakardjieva S, Šubrt J, Pola J 2010 *Journal of Photochemistry and Photobiology A: Chemistry* **215** 164